Advanced Robotics

ISSN: 0169-1864 (Print) 1568-5535 (Online) Journal homepage: https://www.tandfonline.com/loi/tadr20

Kinematic modeling of wheeled mobile robots with slip

Luis Gracia & Josep Tornero

To cite this article: Luis Gracia & Josep Tornero (2007) Kinematic modeling of wheeled mobile robots with slip, Advanced Robotics, 21:11, 1253-1279, DOI: 10.1163/156855307781503763

To link to this article: https://doi.org/10.1163/156855307781503763

Published online: 02 Apr 2012.

Advanced Robotics, Vol. 21, No. 11, pp. 1253–1279 (2007)

Also available online - www.brill.nl/ar

Full paper

Kinematic modeling of wheeled mobile robots with slip

LUIS GRACIA * and JOSEP TORNERO

Department of Systems Engineering and Control, Technical University of Valencia, PO Box 22012, Valencia, Spain

Received 10 October 2006; accepted 16 January 2007

Abstract—This work presents a kinematic modeling method for wheeled mobile robots with slip based on physical principles. First, we present the kinematic modeling of a mobile robot with no-slip considering four types of wheels: fixed, centered orientable, off-centered orientable (castor) and Swedish (also called Mecanum, Ilon or universal). Then, the dynamics of a wheeled mobile robot based on Lagrange formulation are derived and discussed. Next, a quasi-static motion is considered to obtain the kinematic conditions that provide the slip modeling equations. Several types of traction models for the slip between the wheel and the floor are indicated. In particular, for a frictional force linearly dependent on the sliding velocity, the no-slip kinematic equation of the wheeled mobile robot is related, through the weighted least-squares algorithm, with the slip modeling equations. To illustrate the applications of the proposed approach a tricycle vehicle is considered in a real situation. The experimental results obtained for the slip kinematic model are compared with the ones obtained for the well-known Kalman filter.

Keywords: Slippage; sliding friction; traction model; Kalman filter.

1. INTRODUCTION

Wheeled mobile robots (WMR) have been widely studied in the past 15 years. Due to kinematic constraints, many WMR are not integrable (non-holonomic). Therefore, standard techniques (either for kinematic/dynamic modeling) developed for robot manipulators are not directly applicable. This has led to abundant literature dealing with specific simplifications for kinematic models such as trailer-like, etc.

Modeling, which is often a prerequisite to control design and motion planning, is still, however, a relevant issue. Examples of kinematic models for WMR are available in the literature (see Refs [1–12]) among other relevant publications, although not all of them employ a systematic procedure. Most of them assume no-slip [9–12] or lack a proper physical sense in the slip models [4–7]. However,

*To whom correspondence should be addressed. E-mail: luigraca@isa.upv.es

sometimes it is necessary to consider kinematic models with slip, e.g., in a forward solution with redundant sensor information (similarly to the Kalman filter) or with independently over-actuated wheels.

This paper is organized as follows. Section 2 presents the kinematic modeling of a WMR with no-slip considering four types of wheels: fixed, centered orientable (hereinafter orientable), off-centered orientable or castor and Swedish (also called Mecanum, Ilon or universal). In order to provide a proper physical sense to the kinematic models with slip, Section 3 starts from the WMR dynamics and applies three successively approximations: the quasi-static motion model, the slip kinematic model and the weighted least-squares (LS) solution. Also, different traction models, relating the frictional force on the wheel and its sliding velocity, are reviewed and discussed. To illustrate the applications of the proposed approach, Section 4 tests the previously mentioned third kinematic model with slip for a tricycle WMR in a real situation, and compares it with two variants of the Kalman filter and with the classical differential-drive model. Finally, Section 5, Conclusion and Further Work, points out the more outstanding contributions of the present research and suggests extensions.

2. KINEMATIC MODELING WITH NO-SLIP

First, we will introduce some terminology. Assuming horizontal movement, the position of the WMR body is completely specified by three scalar variables (e.g., x, y, θ), referred to in Ref. [9] as WMR posture, $\mathbf{p}$ in vector form. Its first-order time derivative $\dot{\mathbf{p}}$ is called WMR velocity vector and separately (v_x, v_y, ω) WMR velocities [4]. Similarly, for each wheel, wheel velocity vector and wheel velocities are defined.

2.1. Wheel equations

The kinematic modeling of a wheel has been tackled in many researchers as a previous stage for modeling the whole WMR [4–6]. Here, the four common wheels will be considered: fixed, orientable, off-centered orientable or castor and Swedish (Fig. 2). As it is easy to obtain their equations using a vector approach, e.g., see Ref. [13] among many other possibilities, the detailed development will be omitted.

The matrix equation of the castor wheel is:

$$\mathbf{v}_{\text{slip } i} = \begin{pmatrix} \cos(\beta_i + \delta_i) & \sin(\beta_i + \delta_i) & l_i \sin(\beta_i + \delta_i - \alpha_i) - d_i \cos\delta_i & -d_i \cos\delta_i & 0 \\ -\sin(\beta_i + \delta_i) & \cos(\beta_i + \delta_i) & l_i \cos(\beta_i + \delta_i - \alpha_i) + d_i \sin\delta_i & d_i \sin\delta_i & r_i \end{pmatrix} \times \begin{pmatrix} {}^{\bar{\mathrm{R}}}\dot{\mathbf{p}} \\ \dot{\beta}_i \\ \dot{\varphi}_i \end{pmatrix}, \tag{1}$$

where we have used the parameters in Fig. 1a and the variables and constants of Table 1.

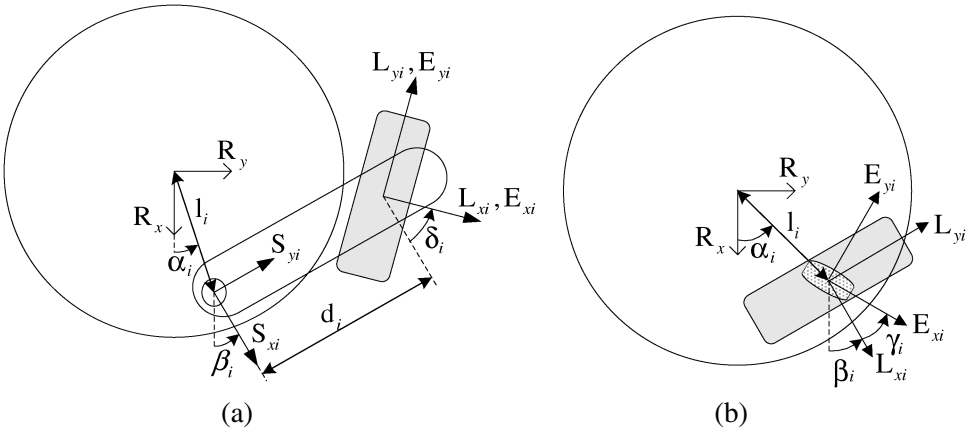

Figure 1. (a) Castor wheel parameters: l_i, d_i, α_i, β_i, δ_i. (b) Swedish wheel parameters: l_i, α_i, β_i, γ_i.

Table 1.
Frames, notation, variables and constants

Symbol	Description
G	global frame attached to the floor with the z-axis perpendicular to the floor surface
R	frame attached to the robot body with the z-axis perpendicular to the floor surface
$\bar{\mathrm{R}}$	frame attached to the floor and coincident with the robot frame R
S_i	frame attached to the steering link of wheel i, with the z-axis coincident with the steering axle and the y-axis parallel to the steering link
L_i	frame attached to wheel i with the x-axis coincident with the wheel rotation axle
E_i	frame attached to the roller of wheel i with the x-axis coincident with its rotation axle
${}^{\mathrm{A}}\mathbf{d}_{\mathrm{B}}$	vector from the origin of frame A to the origin of frame B in coordinate frame A
${}^{\mathrm{A}}\theta_{\mathrm{B}}$	angle between the x-axes of frame B and frame A in coordinate z of frame A
$({}^{\mathrm{A}}\mathbf{v}_{\mathrm{B}}, {}^{\mathrm{A}}\omega_{\mathrm{B}})$	first-order time derivative of vector ${}^{\mathrm{A}}\mathbf{d}_{\mathrm{B}}$ and angle ${}^{\mathrm{A}}\theta_{\mathrm{B}}$, respectively
${}^{\bar{\mathrm{R}}}\dot{\mathbf{p}}$	WMR velocity vector in coordinate frame $\bar{\mathrm{R}}$, equivalent to $({}^{\bar{\mathrm{R}}}v_{\mathrm{R}x}\, {}^{\bar{\mathrm{R}}}v_{\mathrm{R}y}\, {}^{\bar{\mathrm{R}}}\omega_{\mathrm{R}})^{\mathrm{T}}$
${}^{\mathrm{G}}\dot{\mathbf{p}}$	WMR velocity vector in coordinate frame G, equivalent to $({}^{\mathrm{G}}v_{\mathrm{R}x}\, {}^{\mathrm{G}}v_{\mathrm{R}y}\, {}^{\mathrm{G}}\omega_{\mathrm{R}})^{\mathrm{T}}$
$\mathbf{v}_{\mathrm{slip}\ i}$	sliding velocity vector of the wheel in coordinate frame E_i
$\dot{\beta}_i$	angular velocity of the steering link with respect to the WMR
$(\dot{\varphi}_i, \dot{\varphi}_{\mathrm{r}i})$	rotation velocity of the wheel and the rollers in coordinate x of frames L_i and E_i
$(r_i, r_{\mathrm{r}i})$	wheel equivalent radius and roller radius

The matrix equation of the orientable wheel can be obtained from (1) with $d_i = \delta_i = 0$:

$$\mathbf{v}_{\mathrm{slip}\ i} = \begin{pmatrix} \cos\beta_i & \sin\beta_i & l_i \sin(\beta_i - \alpha_i) & 0 \\ -\sin\beta_i & \cos\beta_i & l_i \cos(\beta_i - \alpha_i) & r_i \end{pmatrix} \begin{pmatrix} {}^{\bar{\mathrm{R}}}\dot{\mathbf{p}} \\ \dot{\varphi}_i \end{pmatrix}. \tag{2}$$

The previous equation is also valid for fixed wheels, where the angle β_i is constant.

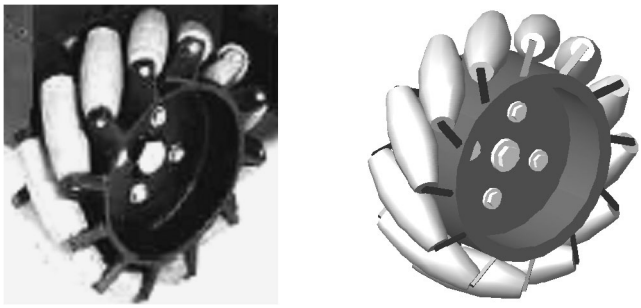

Figure 2. Swedish wheel (also called Mecanum, Ilon or universal) with rollers at 45°.

The matrix equation of the Swedish wheel (Fig. 2) is (3) where we have used the parameters in Fig. 1b and the variables and constants of Table 1.

$$\mathbf{v}_{\text{slip } i} = \begin{pmatrix} \cos(\beta_i + \gamma_i) & \sin(\beta_i + \gamma_i) & l_i \sin(\beta_i + \gamma_i - \alpha_i) & r_i \sin\gamma_i & 0 \\ -\sin(\beta_i + \gamma_i) & \cos(\beta_i + \gamma_i) & l_i \cos(\beta_i + \gamma_i - \alpha_i) & r_i \cos\gamma_i & r_{\text{ri}} \end{pmatrix} \times \begin{pmatrix} {}^{\bar{\text{R}}}\dot{\mathbf{p}} \\ \dot{\varphi}_i \\ \dot{\varphi}_{\text{ri}} \end{pmatrix}, \tag{3}$$

Note that, in the previous wheel equations, the instantaneously coincident frame $\bar{\text{R}}$ avoids dependency on the global stationary frame G [4]. The WMR velocity vector in coordinate frame G is:

$${}^{\text{G}}\dot{\mathbf{p}} = \begin{pmatrix} \mathbf{Rot}({}^{\text{G}}\theta_{\text{R}}) & \begin{matrix} 0 \\ 0 \end{matrix} \\ \begin{matrix} 0 & 0 \end{matrix} & 1 \end{pmatrix} {}^{\bar{\text{R}}}\dot{\mathbf{p}} = \mathbf{Rot}_Z({}^{\text{G}}\theta_{\text{R}}) {}^{\bar{\text{R}}}\dot{\mathbf{p}}, \tag{4}$$

where $\mathbf{Rot}_Z(x)$ is a three-dimensional z-axis rotation of x and $\mathbf{Rot}(x)$ a two-dimensional rotation matrix:

$$\mathbf{Rot}(x) = \begin{pmatrix} \cos x & -\sin x \\ \sin x & \cos x \end{pmatrix}, \tag{5}$$

with the properties $\mathbf{Rot}^{-1}(x) = \mathbf{Rot}^{\text{T}}(x) = \mathbf{Rot}(-x)$.

2.2. Kinematic equation of the WMR

Once the type of WMR wheels and their equations (through the corresponding wheel parameters: $r_i, r_{\text{ri}}, l_i, d_i, \alpha_i, \beta_i, \delta_i, \gamma_i$) are established, a compound global kinematic equation for the WMR may be defined. For that purpose, using (1),

Table 2.
New variables and constants in (6)

Symbol	Description
N	number of wheels of the WMR
$\mathbf{v}_{\text{slip}}$	vector of all the sliding velocities $\mathbf{v}_{\text{slip }i}$
$\dot{\mathbf{q}}_{\text{w}i}$	vector with all the velocities of the wheel i
$(\dot{\mathbf{q}}_{\text{w}}, {}^{\bar{\text{R}}}\dot{\mathbf{q}})$	vector of all the wheel velocities and vector of all velocities, respectively
$\mathbf{A}_{\text{p}i}/\mathbf{A}_{\text{w}i}$	multiplying matrix of the WMR/wheel velocity vector in (1), (2) and (3)
$\mathbf{A}_{\text{p}}/\mathbf{A}_{\text{w}}$	association of the WMR/wheel multiplying matrices

(2) and (3) the compound WMR kinematic equation is derived:

$$\begin{aligned}\mathbf{v}_{\text{slip}} &= \begin{pmatrix} \mathbf{v}_{\text{slip }1} \\ \vdots \\ \mathbf{v}_{\text{slip }N} \end{pmatrix} = \begin{pmatrix} \mathbf{A}_{\text{p}1} & \mathbf{A}_{\text{w}1} & \cdots & 0 \\ \vdots & \vdots & \ddots & \vdots \\ \mathbf{A}_{\text{p}N} & 0 & \cdots & \mathbf{A}_{\text{w}N} \end{pmatrix} \begin{pmatrix} {}^{\bar{\text{R}}}\dot{\mathbf{p}} \\ \dot{\mathbf{q}}_{\text{w}1} \\ \vdots \\ \dot{\mathbf{q}}_{\text{w}N} \end{pmatrix} \\ &= \begin{pmatrix} \mathbf{A}_{\text{p}} & \mathbf{A}_{\text{w}} \end{pmatrix} \begin{pmatrix} \dot{\mathbf{p}} \\ \dot{\mathbf{q}}_{\text{w}} \end{pmatrix} = {}^{\bar{\text{R}}}\mathbf{A}\,{}^{\bar{\text{R}}}\dot{\mathbf{q}}, \end{aligned} \tag{6}$$

with the meaning of new variables and constants of Table 2. It is possible to redefine (6) as:

$$\mathbf{v}_{\text{slip}} = \begin{pmatrix} \mathbf{A}_{\text{p}}\mathbf{Rot}_Z(-{}^{\text{G}}\theta_{\text{R}}) & \mathbf{A}_{\text{w}} \end{pmatrix} \begin{pmatrix} {}^{\text{G}}\dot{\mathbf{p}} \\ \dot{\mathbf{q}}_{\text{w}} \end{pmatrix} = {}^{\text{G}}\mathbf{A}\,{}^{\text{G}}\dot{\mathbf{q}}. \tag{7}$$

2.3. Kinematic modeling of WMR with no-slip

Under the no-slip condition (6) or (7) become:

$$\mathbf{A}\dot{\mathbf{q}} = \mathbf{0}, \tag{8}$$

where the left superscript is omitted. Therefore, the kinematic solution for the velocity vector $\dot{\mathbf{q}}$ belongs to the null space of WMR matrix $\mathbf{A}$, i.e.:

$$\dot{\mathbf{q}} \in \mathcal{N}(\mathbf{A}) \quad \longrightarrow \quad \dot{\mathbf{q}} = \mathbf{B}\boldsymbol{\eta}, \tag{9}$$

where the matrix $\mathbf{B}$ forms a basis of $\mathcal{N}(\mathbf{A})$, $\boldsymbol{\eta}$ is an m-dimensional vector representing the WMR mobility and m is the WMR mobility degree given by the nullity of $\mathbf{A}$ (rank-nullity theorem):

$$m = \dim(\boldsymbol{\eta}) = \dim(\mathcal{N}(\mathbf{A})) = \dim(\dot{\mathbf{q}}) - \operatorname{rank}(\mathbf{A}) = k - g. \tag{10}$$

In order to use variables with physical meaning, the mobility vector $\boldsymbol{\eta}$ should be replaced with a set of freely assigned velocities. Depending on whether wheel velocities or WMR velocities are chosen, a forward or inverse kinematic model is obtained. If a mix of both types of velocities is chosen a mixed solution is achieved.

To check if an m-set of velocities $\dot{\mathbf{q}}_{\mathrm{a}}$ can be assigned, it must be verified that the determinant of the submatrix they define in (9) is non-zero, i.e.:

$$\begin{pmatrix} \dot{\mathbf{q}}_{\mathrm{na}} \\ \dot{\mathbf{q}}_{\mathrm{a}} \end{pmatrix} = \begin{pmatrix} \mathbf{B}_{\mathrm{na}} \\ \mathbf{B}_{\mathrm{a}} \end{pmatrix} \boldsymbol{\eta} \tag{11}$$

$$\text{if} \quad |\mathbf{B}_{\mathrm{a}}| \neq 0 \quad \longrightarrow \quad \dot{\mathbf{q}}_{\mathrm{na}} = \mathbf{B}_{\mathrm{na}} \mathbf{B}_{\mathrm{a}}^{-1} \dot{\mathbf{q}}_{\mathrm{a}}, \tag{12}$$

where $\dot{\mathbf{q}}_{\mathrm{na}}$ are the remaining non-assigned velocities of $\dot{\mathbf{q}}$ and the singularity of $\mathbf{B}_{\mathrm{a}}$ for particular configurations characterizes the WMR singularity [13].

Alternatively to the previous procedure, based upon the null space concept, it is possible to apply another method, based on separating the assigned velocities in (8):

$$\mathbf{A}_{\mathrm{na}} \dot{\mathbf{q}}_{\mathrm{na}} = -\mathbf{A}_{\mathrm{a}} \dot{\mathbf{q}}_{\mathrm{a}}. \tag{13}$$

To check if an m-set of velocities could be assigned $\dot{\mathbf{q}}_{\mathrm{a}}$, it must be verified that matrix $\mathbf{A}_{\mathrm{na}}$ is, in general, of full rank g:

$$\mathrm{rank}(\mathbf{A}_{\mathrm{na}}) = \mathrm{rank}(\mathbf{A}) = g. \tag{14}$$

3. KINEMATIC MODELING WITH SLIP

3.1. Introduction

Several publications have tackled the kinematic modeling of WMR with slip. In reference [4] considers a kinematic solution with redundant information ($\dim(\dot{\mathbf{q}}_{\mathrm{a}}) > m$) applying left pseudoinverse to (13):

$$\dot{\mathbf{q}}_{\mathrm{na}} = -(\mathbf{A}_{\mathrm{na}}^{\mathrm{T}} \mathbf{A}_{\mathrm{na}})^{-1} \mathbf{A}_{\mathrm{na}}^{\mathrm{T}} \mathbf{A}_{\mathrm{a}} \dot{\mathbf{q}}_{\mathrm{a}}. \tag{15}$$

Nevertheless, this (LS) solution proposed in Ref. [4] violates, as pointed out [6] with a numerical example, the kinematic constraints (i.e., rigid body model) of the mobile robot. This violation is produced, unlike the explanation given in Ref. [6], because it considers a wheel equation with three scalar elements, instead of two like (1) and (2) (the Swedish wheel is not considered). The additional third scalar equation relates wheel steering velocity $\dot{\beta}_i$ with WMR angular velocity ${}^{\bar{\mathrm{R}}}\omega_{\mathrm{R}}$ through the useless wheel velocity ${}^{\overline{\mathrm{E}i}}\omega_{\mathrm{E}i}$ (neither sensed nor actuated):

$${}^{\bar{\mathrm{R}}}\omega_{\mathrm{R}} = {}^{\overline{\mathrm{E}i}}\omega_{\mathrm{E}i} - \dot{\beta}_i. \tag{16}$$

As a result, when the LS algorithm is computed this scalar equation is not guaranteed, which is not acceptable since this constraint must be always satisfied, not like the other two that may allow slip. For example, a fixed or Swedish wheel has null steering velocity $\dot{\beta}_i$ and, therefore, its angular velocity ${}^{\overline{\mathrm{E}i}}\omega_{\mathrm{E}i}$ must be always be equal to WMR angular velocity ${}^{\bar{\mathrm{R}}}\omega_{\mathrm{R}}$.

Meanwhile, Ref. [6] considers explicitly the sliding velocities, in a similar way to (6), and applies the weighted right pseudoinverse in order to compute non-assigned wheel velocities $\dot{\mathbf{q}}_{\mathrm{w\_na}}$ and sliding velocities $\mathbf{v}_{\mathrm{slip}}$. Thus, the algorithm

minimizes the weighted Euclidean norm of $(\dot{\mathbf{q}}_{\mathrm{w\_na}}\mathbf{v}_{\mathrm{slip}})^{\mathrm{T}}$, which does not have a defined physical sense. Reference [7] considers a four orientable wheel WMR with the steering and rotation velocities of each wheel measured. It uses several expressions (that relate the wheel velocities with the WMR velocities and some slip variables) together with the extended Kalman filter (EKF) to make an adaptive state estimation. Nevertheless, the mentioned slip relationships are completely ad-hoc and do not present a rigorous justification. In the same way, Ref. [8] develops a particular kinematic model for an articulated WMR, with a front and rear body, that includes the slip angle of each body. These angles and the WMR posture are estimated with an EKF.

Reference [5] proposes minimizing the dissipation functional P_{dis} produced by Coulomb frictional forces $\mathbf{F}_{\mathrm{fric\_c}i}$ with dynamic friction coefficients μ_i:

$$\mathbf{F}_{\mathrm{fric\_c}i} = -\mu_i \frac{\mathbf{v}_{\mathrm{slip}\ i}}{|\mathbf{v}_{\mathrm{slip}\ i}|} \tag{17}$$

$$P_{\mathrm{dis}} = -\sum_{i=1}^{N} (\mathbf{F}_{\mathrm{fric\_c}i}\mathbf{v}_{\mathrm{slip}\ i}) = -\sum_{i=1}^{N} (\mathbf{F}^{\mathrm{T}}_{\mathrm{fric\_c}i}\mathbf{v}_{\mathrm{slip}\ i}). \tag{18}$$

It is shown that a minimization with respect to WMR velocity vector $\dot{\mathbf{p}}$ is equivalent to equilibrium of forces and moments, and characterizes a quasi-static motion (null accelerations). Nevertheless, the minimization process does not follow a correct solution for a generic frictional force. This will be explained with a very simple example, but with the same underlying principles. Let us consider a free block sliding in one direction on a surface with a generic frictional force:

$$F_{\mathrm{fric\_b}} = -f(|v_{\mathrm{b}}|)\frac{v_{\mathrm{b}}}{|v_{\mathrm{b}}|}, \tag{19}$$

where v_{b} is the non-zero block (sliding) velocity and f the frictional force module dependent on the sliding velocity module. The dissipation functional becomes:

$$P_{\mathrm{dis\_b}} = -F_{\mathrm{fric\_b}}v_{\mathrm{b}} = |v_{\mathrm{b}}|f(|v_{\mathrm{b}}|), \tag{20}$$

and its minimization with respect to v_{b} is:

$$\frac{\mathrm{d}P_{\mathrm{dis\_b}}}{\mathrm{d}v_{\mathrm{b}}} = \frac{\mathrm{d}P_{\mathrm{dis\_b}}}{\mathrm{d}|v_{\mathrm{b}}|}\frac{\mathrm{d}|v_{\mathrm{b}}|}{\mathrm{d}v_{\mathrm{b}}} = \left(f(|v_{\mathrm{b}}|) + |v_{\mathrm{b}}|\frac{\mathrm{d}f(|v_{\mathrm{b}}|)}{\mathrm{d}|v_{\mathrm{b}}|}\right)\frac{v_{\mathrm{b}}}{|v_{\mathrm{b}}|} = 0. \tag{21}$$

The solution for quasi-static motion is:

$$F_{\mathrm{fric\_b}} = -f(|v_{\mathrm{b}}|)\frac{v_{\mathrm{b}}}{|v_{\mathrm{b}}|} = 0. \tag{22}$$

Comparing the two previous expressions:

$$f(|v_{\mathrm{b}}|) + |v_{\mathrm{b}}|\frac{\mathrm{d}f(|v_{\mathrm{b}}|)}{\mathrm{d}|v_{\mathrm{b}}|} = kf(|v_{\mathrm{b}}|), \tag{23}$$

where k is a generic constant. The condition (23) is satisfied, for example, by a frictional force module f: 1, $|v_b|$, $|v_b|^2$, $|v_b|^3$, ..., but not by a frictional force module f: $1 + |v_b|$, $1 + |v_b|^2$, $|v_b| + |v_b|^2$, ...

The procedure for a WMR with several sliding wheels is analogous to that just presented, but with two-dimensional (2-D) frictional forces and sliding velocities. Then it is concluded that the minimization of the dissipation functional does not produce in general the equations of the quasi-static motion. Moreover, it would not take into account other possible external forces, e.g., the block with a tangential weight component on an inclined plane. In fact, in the presented example some external force should be considered in (22) to produce a non-zero sliding velocity v_b.

3.2. Dynamics with Lagrange formulation

The main inconvenience of the slip kinematic modeling methods described in the previous subsection is the lack of a proper physical sense. In order to overcome this, here we will consider as a starting point the WMR dynamics with Lagrange formulation. Afterwards, this dynamic approach will be restricted to a kinematic, quasi-static motion.

The general Lagrange equations for a finite-dimensional dynamic system are given by:

$$\frac{\mathrm{d}}{\mathrm{d}t}\left(\frac{\partial T}{\partial \dot{\mathbf{q}}}\right) - \frac{\partial T}{\partial \mathbf{q}} = \mathbf{Q}, \tag{24}$$

where $\mathbf{q}$ is the generalized coordinate vector (in our case equivalent to ${}^{\mathrm{G}}\mathbf{q}$), $\mathbf{Q}$ is the generalized force vector (that includes the conservative forces) and T is the kinetic energy. The generalized force vector is:

$$\mathbf{Q} = \sum_i \mathbf{F}_i \cdot \frac{\partial \mathbf{r}_i}{\partial \mathbf{q}} = \sum_i \mathbf{F}_i^{\mathrm{T}} \frac{\partial \mathbf{v}_i}{\partial \dot{\mathbf{q}}}, \tag{25}$$

where $\mathbf{F}_i$ are the acting forces/torques and $\mathbf{F}_i \cdot \delta\mathbf{r}_i$ the corresponding virtual work compatible with the constraints of the system. For example, the weight (conservative force) of a WMR with a horizontal movement produces no virtual work. In our case the generalized force vector is:

$$\mathbf{Q} = \sum_{i=1}^{N} \tau_{\mathrm{r}i} \frac{\partial \dot{\varphi}_i}{\partial \dot{\mathbf{q}}} + \sum_{i=1}^{N_{\mathrm{o}}} \tau_{\mathrm{o}si} \frac{\partial \dot{\beta}_{\mathrm{o}i}}{\partial \dot{\mathbf{q}}} + \sum_{i=1}^{N_{\mathrm{c}}} \tau_{\mathrm{c}si} \frac{\partial \dot{\beta}_{\mathrm{c}i}}{\partial \dot{\mathbf{q}}} + \sum_{i=1}^{N} \mathbf{F}_{\mathrm{fric}\ i}^{\mathrm{T}} \frac{\partial \mathbf{v}_{\mathrm{slip}\ i}}{\partial \dot{\mathbf{q}}}, \tag{26}$$

with the meaning of new variables and constants of Table 3.

Note that a frictional force $\mathbf{F}_{\mathrm{fric}\ i}$ in the opposite direction of the sliding velocity $\mathbf{v}_{\mathrm{slip}\ i}$ produces a negative sign of the last term of (26), what indicates a dissipative work. Expression (26), using (7), is:

$$\mathbf{Q} = \boldsymbol{\tau} + \mathbf{F}_{\mathrm{fric}}^{\mathrm{T}}\mathbf{A} = \boldsymbol{\tau} + \mathbf{A}^{\mathrm{T}}\mathbf{F}_{\mathrm{fric}}, \tag{27}$$

Table 3.
New variables and constants in (26) and (28)

Symbol	Description
$N_o/N_c/N_s$	number of orientable/castor/Swedish wheels of the WMR
τ_{ri}	rotation torque of wheel I
τ_{osi}/τ_{csi}	steering torque of the orientable/castor wheel i
$\dot{\beta}_{oi}/\dot{\beta}_{ci}$	steering velocity of the orientable/castor wheel i
$\mathbf{F}_{\text{fric } i}$	Frictional force on the wheel i in coordinate frame E_i
(M_T, M_{ci})	mass of the WMR* (WMR without castor wheels) and mass of all castor wheel i
I_T	moment of inertia of the WMR* with respect to a Z axle crossing its MC
I_{ri}	moment of inertia of wheel i respect to its rotation axle
I_{rri}	moment of inertia of the roller of Swedish wheel i
I_{osi}/I_{csi}	moment of inertia of all (steering link included) orientable/castor wheel I with respect to a Z axle crossing its MC
${}^G\mathbf{v}_{MC}$	velocity of the MC of the WMR* in coordinate frame G
${}^G\mathbf{v}_{mci}$	velocity of the MC of castor wheel i

where $\boldsymbol{\tau}$ is a global torque vector and F_{fric} is the grouped frictional forces. It is interesting to remark that the last term of (27) would also be present in (24) if no-slip is considered because of the constraints given by (8) and frictional forces $\mathbf{F}_{\text{fric } i}$ would be the opposite of Lagrange multipliers λ [14].

Meanwhile, the kinetic energy of the WMR is:

$$\begin{aligned} T = {} & \frac{1}{2}\left(M_T({}^G v_{MCx}^2 + {}^G v_{MCy}^2) + I_T{}^{\bar{R}}\omega_R^2 + \sum_{i=1}^{N} I_{ri}\dot{\varphi}_i^2 + \sum_{i=1}^{N_s} I_{rri}\dot{\varphi}_{ri}^2 \right) \\ & + \frac{1}{2}\sum_{i=1}^{N_c}\left(M_{ci}\left({}^G v_{mcix}^2 + {}^G v_{mciy}^2\right) + I_{csi}(\dot{\beta}_{ci} + {}^{\bar{R}}\omega_R)^2 \right) \\ & + \frac{1}{2}\sum_{i=1}^{N_o}\left(I_{osi}(\dot{\beta}_{oi}^2 + 2\dot{\beta}_{oi}{}^{\bar{R}}\omega_R) \right), \end{aligned} \tag{28}$$

with the meaning of variables and constants of Table 3. Note that (28) takes into account that the mass center (MC) of all the centered wheels (fixed, orientable and Swedish) does not change with respect to the WMR body. Although no motion is considered for the z-axis in (28), the WMR linear acceleration ${}^G\dot{\mathbf{v}}_{MC}$ and the body reaction torques due to τ_{ri} redistribute the normal forces on the wheels.

For convenience, the origin of the body frame R will be located on the MC of the WMR*, so that ${}^G\mathbf{v}_{MC} = {}^G\mathbf{v}_R$. It is easy to obtain the following relationship from Fig. 1a:

$${}^G\mathbf{d}_{mci} = {}^G\mathbf{d}_R + \begin{pmatrix} l_i\cos({}^G\theta_R + \alpha_i) - d_{mci}\sin({}^G\theta_R + \beta_i) \\ l_i\sin({}^G\theta_R + \alpha_i) + d_{mci}\cos({}^G\theta_R + \beta_i) \end{pmatrix}, \tag{29}$$

where d_{mci} is the distance from the z-axis of frame S to the MC of castor wheel i.

The first- and second-order time derivative of ${}^{\mathrm{G}}\mathbf{d}_{\mathrm{mc}i}$ are:

$$ {}^{\mathrm{G}}\mathbf{v}_{\mathrm{mc}i} = {}^{\mathrm{G}}\mathbf{v}_{\mathrm{R}} + \mathbf{f}_{1i}\,{}^{\bar{\mathrm{R}}}\omega_{\mathrm{R}} + \mathbf{f}_{2i}\dot{\beta}_i \tag{30} $$

$$ {}^{\mathrm{G}}\dot{\mathbf{v}}_{\mathrm{mc}i} = {}^{\mathrm{G}}\dot{\mathbf{v}}_{\mathrm{R}} + \mathbf{f}_{3i}\,{}^{\bar{\mathrm{R}}}\dot{\omega}_{\mathrm{R}} + \mathbf{f}_{4i}\ddot{\beta}_i + \mathbf{f}_{5i}\,{}^{\bar{\mathrm{R}}}\omega_{\mathrm{R}}^2 + \mathbf{f}_{6i}\dot{\beta}_i^2 + 2\mathbf{f}_{7i}\,{}^{\bar{\mathrm{R}}}\omega_{\mathrm{R}}\dot{\beta}_i, \tag{31} $$

where f_{ji} is a function of l_i, $d_{\mathrm{mc}i}$, α_i, ${}^{\mathrm{G}}\theta_{\mathrm{R}}$ and β_i.

The WMR dynamics (24), taking into account {(1)–(7), (26)–(28) and (30)}, results in:

$$ \left(M_{\mathrm{T}} + \sum_{i=1}^{N_{\mathrm{c}}} M_{\mathrm{c}i}\right){}^{\mathrm{G}}\dot{\mathbf{v}}_{\mathrm{R}} = \mathbf{Rot}({}^{\mathrm{G}}\theta_{\mathrm{R}}) \sum_{i=1}^{N} \mathbf{Rot}({}^{\mathrm{R}}\theta_{\mathrm{E}i})\mathbf{F}_{\mathrm{fric}\ i} \tag{32} $$

$$ \begin{aligned} &\left(I_{\mathrm{T}} + \sum_{i=1}^{N_{\mathrm{c}}} I_{\mathrm{cs}i}\right){}^{\bar{\mathrm{R}}}\dot{\omega}_{\mathrm{R}} + \sum_{i=1}^{N_{\mathrm{c}}} M_{\mathrm{c}i}\mathbf{f}_{1i}^{\mathrm{T}}\,{}^{\mathrm{G}}\dot{\mathbf{v}}_{\mathrm{mc}i} + \sum_{i=1}^{N_{\mathrm{c}}} I_{\mathrm{cs}i}\ddot{\beta}_{\mathrm{c}i} + \sum_{i=1}^{N_{\mathrm{o}}} I_{\mathrm{os}i}\ddot{\beta}_{\mathrm{o}i} \\ &\quad = \sum_{i=1}^{N}\left({}^{\mathrm{R}}\mathbf{d}_{\mathrm{E}i} \times \begin{pmatrix} \mathbf{Rot}({}^{\mathrm{R}}\theta_{\mathrm{E}i})\mathbf{F}_{\mathrm{fric}\ i} \\ 0 \end{pmatrix}\right) \cdot \begin{pmatrix} 0 \\ 0 \\ 1 \end{pmatrix} \end{aligned} \tag{33} $$

$$ I_{\mathrm{cs}j}({}^{\bar{\mathrm{R}}}\dot{\omega}_{\mathrm{R}} + \ddot{\beta}_{\mathrm{c}j}) + M_{\mathrm{c}j}\mathbf{f}_{2j}^{\mathrm{T}}\,{}^{\mathrm{G}}\dot{\mathbf{v}}_{\mathrm{mc}j} = \tau_{\mathrm{cs}j} - \left({}^{\mathrm{E}j}\mathbf{d}_{\mathrm{S}j} \times \begin{pmatrix} \mathbf{F}_{\mathrm{fric}\ j} \\ 0 \end{pmatrix}\right) \cdot \begin{pmatrix} 0 \\ 0 \\ 1 \end{pmatrix} \tag{34} $$

$$ I_{\mathrm{os}j}(\ddot{\beta}_{\mathrm{o}j} + {}^{\bar{\mathrm{R}}}\dot{\omega}_{\mathrm{R}}) = \tau_{\mathrm{os}j} \tag{35} $$

$$ I_{\mathrm{r}j}\ddot{\varphi}_j = \tau_{\mathrm{r}j} + r_j\,(\,\sin\gamma_j \quad \cos\gamma_j\,)\,\mathbf{F}_{\mathrm{fric}\ j} \tag{36} $$

$$ I_{\mathrm{rr}j}\ddot{\varphi}_{\mathrm{r}j} = r_{\mathrm{r}j}\,(\,0 \quad 1\,)\,\mathbf{F}_{\mathrm{fric}\ j}, \tag{37} $$

with j from 1 to N_{c} (34), to N_{o} (35), to N (36) or to N_{s} (37).

3.3. Traction model

The a component, either lateral x or longitudinal y, of the tractive frictional force on the wheel is:

$$ F_{\mathrm{fric}\ a} = -\mu_a F_{\mathrm{N}}, \tag{38} $$

where F_{N} is the normal force or reaction at the wheel contact point and μ_a the adhesion or friction coefficient. The adhesion coefficient is a function of the wheel dynamics and tractive conditions. It depends on quantities such as the sliding velocity of the wheel, the surface roughness, the wheel material, etc. In general, there are four static friction phenomena, i.e., static friction, Coulomb friction (dynamic friction), viscous friction and Stribeck effect, and three dynamic friction phenomena, i.e., Dahl effect, rising static friction and frictional lag. The static friction models, also referred to as the steady-state models, have a static dependency on the sliding velocity through the so-called Stribeck curve [22]. Meanwhile the dynamic friction models incorporate a spring-like behavior for small forces.

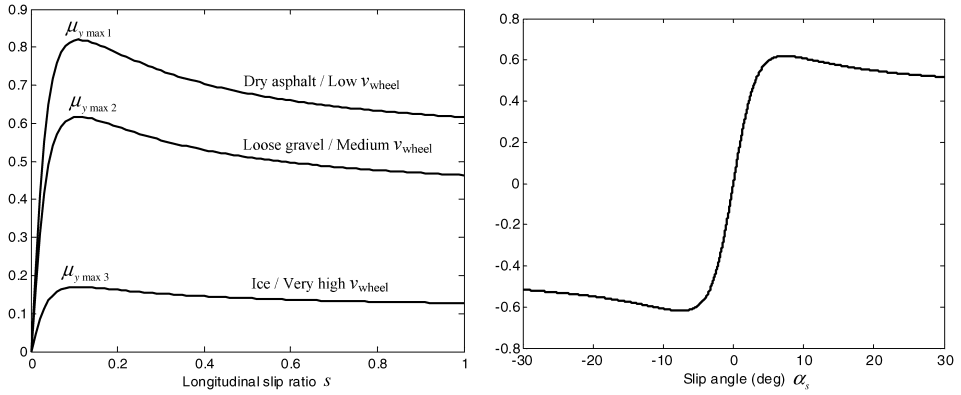

Figure 3. Static curve for the adhesion coefficients. (a) Longitudinal adhesion coefficient μ (b) Lateral adhesion coefficient μ.

Examples of dynamic models are Dahl [23], Bliman-Sorine [24] and LuGre [25]. Both static and dynamic models may assume a wheel with lumped or distributed frictional force.

Many models have been developed under the static framework [15–18] to relate wheel longitudinal adhesion coefficient μ_y and longitudinal slip ratio s (39) for pure longitudinal slip (Fig. 3a). Those models are also used to relate the wheel lateral adhesion coefficient μ_x and the slip angle α_s (39) for a pure lateral slip (Fig. 3b). All these models have an approximated straight line behavior (Fig. 3) for small slip ratio/angle that is characterized by the slope, commonly referred to as the longitudinal stiffness or slip slope. For example, a stiff tire gives a large slip slope. For a combined slip motion we must consider the coupling properties of the friction components, so it is achieved a further representation of a pure longitudinal/lateral slip [19, 27, 28]:

$$s = \frac{(\dot{\varphi}\mathrm{r} - v_{\mathrm{wheel}})}{\max(|\dot{\varphi}r|, |v_{\mathrm{wheel}}|)} = \frac{v_{\mathrm{slip}}}{\max(|\dot{\varphi}r|, |v_{\mathrm{wheel}}|)}, \quad \alpha_{\mathrm{s}} = \operatorname{atan}\left(\frac{v_{\mathrm{slip}}}{v_{\mathrm{wheel}}}\right). \tag{39}$$

3.4. Quasi-static motion model

In order to explain the approach of this point, let us consider the second-order dynamic model (40) with **x** the unknown variables (positions) and **u** the input vector (forces/torques):

$$\mathbf{f}(\ddot{\mathbf{x}}, \dot{\mathbf{x}}, \mathbf{x}, \mathbf{u}) = 0 \rightarrow \ddot{\mathbf{x}}. \tag{40}$$

The previous expression is used to compute instantaneously $\ddot{\mathbf{x}}$ and could be used to compute the stationary value $\dot{\mathbf{x}}_\infty$ of a quasi-static (null accelerations) situation:

$$\mathbf{f}(\mathbf{0}, \dot{\mathbf{x}}_\infty, \mathbf{x}, \mathbf{u}) = 0 \rightarrow \dot{\mathbf{x}}_\infty. \tag{41}$$

The situation (40) corresponds to the dynamic model of the subsection 3.2 (together with subsection 3.3), where the computed variables are $\ddot{\mathbf{q}}$ and the input variables are $\boldsymbol{\tau}$. Meanwhile, the situation (41) corresponds to a quasi-static model with the computed variables $\dot{\mathbf{q}}_\infty$ and the inputs $\boldsymbol{\tau}$. This second situation is tackled at this point. If we define the WMR quasi-static motion as:

$$^{\mathrm{G}}\ddot{\mathbf{q}} = 0 \rightarrow {}^{\mathrm{G}}\dot{v}_{\mathrm{R}x} = {}^{\mathrm{G}}\dot{v}_{\mathrm{R}y} = {}^{\bar{\mathrm{R}}}\dot{\omega}_{\mathrm{R}} = \ddot{\beta}_{\mathrm{c}j} = \ddot{\beta}_{\mathrm{o}j} = \ddot{\varphi}_j = \ddot{\varphi}_{\mathrm{r}j} = 0, \tag{42}$$

it implies that the WMR* has a uniform rectilinear motion $^{\mathrm{G}}\dot{\mathbf{v}}_{\mathrm{R}} = \mathbf{0}$ with a constant angular velocity $^{\bar{\mathrm{R}}}\dot{\omega}_{\mathrm{R}} = 0$. Nevertheless, because of the fact that for this motion the WMR* orientation in coordinate frame G $^{\mathrm{G}}\theta_{\mathrm{R}}$ would vary, there would not be in general a stationary value $\dot{\mathbf{x}}_\infty$ for $(^{\mathrm{G}}\mathbf{v}_{\mathrm{R}}, {}^{\bar{\mathrm{R}}}\omega_{\mathrm{R}}, \dot{\varphi}_j, \ldots)$. For example, the WMR based on two aligned fixed wheels (differential-drive WMR) cannot develop a rectilinear motion at a constant angular velocity. Then, we must consider the WMR quasi-static motion with respect to the coincident frame $\bar{\mathrm{R}}$:

$$^{\bar{\mathrm{R}}}\ddot{\mathbf{q}} = 0 \quad \rightarrow \quad {}^{\bar{\mathrm{R}}}\dot{v}_{\mathrm{R}x} = {}^{\bar{\mathrm{R}}}\dot{v}_{\mathrm{R}y} = {}^{\bar{\mathrm{R}}}\dot{\omega}_{\mathrm{R}} = \ddot{\beta}_{\mathrm{c}j} = \ddot{\beta}_{\mathrm{o}j} = \ddot{\varphi}_j = \ddot{\varphi}_{\mathrm{r}j} = 0, \tag{43}$$

what implies that the WMR* has a uniform curvilinear motion, characterized by $^{\bar{\mathrm{R}}}\mathbf{v}_{\mathrm{R}}$ and $^{\bar{\mathrm{R}}}\omega_{\mathrm{R}}$, with a constant angular velocity $^{\bar{\mathrm{R}}}\omega_{\mathrm{R}}$. For this motion the relationship (44), obtained from (4), has to be substituted in (31) and (32):

$$^{\mathrm{G}}\dot{\mathbf{v}}_{\mathrm{R}} = \mathbf{Rot}(^{\mathrm{G}}\theta_{\mathrm{R}})\,{}^{\bar{\mathrm{R}}}\dot{\mathbf{v}}_{\mathrm{R}} + {}^{\bar{\mathrm{R}}}\omega_{\mathrm{R}}(\partial\mathbf{Rot}(^{\mathrm{G}}\theta_{\mathrm{R}})/\partial\,{}^{\mathrm{G}}\theta_{\mathrm{R}})\,{}^{\bar{\mathrm{R}}}\mathbf{v}_{\mathrm{R}}. \tag{44}$$

Under the conditions (43) all the left sides, of the dynamic equations (32)–(37) are zero except for the centripetal term $^{\bar{\mathrm{R}}}\omega_{\mathrm{R}}\,{}^{\bar{\mathrm{R}}}\mathbf{v}_{\mathrm{R}}$ of $^{\mathrm{G}}\dot{\mathbf{v}}_{\mathrm{R}}$ in (44), and the centrifugal $(^{\bar{\mathrm{R}}}\omega_{\mathrm{R}}^2, \dot{\beta}_i^2)$ and the Coriolis $(^{\bar{\mathrm{R}}}\omega_{\mathrm{R}}\dot{\beta}_i)$ terms of $^{\mathrm{G}}\dot{\mathbf{v}}_{\mathrm{mc}i}$ in (31). If the non-zero terms of the castor wheels due to (31) are neglected in (33) and (34), e.g., the mass of the castor wheels M_{ci} is very small, the dynamic equations are transformed into the following quasi-static motion equations:

$$\left(M_{\mathrm{T}} + \sum_{i=1}^{N_{\mathrm{c}}} M_{ci}\right) {}^{\bar{\mathrm{R}}}\omega_{\mathrm{R}} \begin{pmatrix} 0 & -1 \\ 1 & 0 \end{pmatrix} {}^{\bar{\mathrm{R}}}\mathbf{v}_{\mathrm{R}} = \sum_{i=1}^{N} \mathbf{Rot}(^{\mathrm{R}}\theta_{\mathrm{E}i})\mathbf{F}_{\mathrm{fric}\ i} \tag{45}$$

$$0 = \sum_{i=1}^{N} \left({}^{\mathrm{R}}\mathbf{d}_{\mathrm{E}i} \times \begin{pmatrix} \mathbf{Rot}(^{\mathrm{R}}\theta_{\mathrm{E}i})\mathbf{F}_{\mathrm{fric}\ i} \\ 0 \end{pmatrix} \right) \cdot (0 \quad 0 \quad 1)^{\mathrm{T}} \tag{46}$$

$$0 = \tau_{\mathrm{cs}j} - \left({}^{\mathrm{E}j}\mathbf{d}_{\mathrm{S}j} \times \begin{pmatrix} \mathbf{F}_{\mathrm{fric}\ j} \\ 0 \end{pmatrix} \right) \cdot (0 \quad 0 \quad 1)^{\mathrm{T}} \tag{47}$$

$$0 = \tau_{\mathrm{os}j} \tag{48}$$

$$0 = \tau_{\mathrm{r}j} + r_j\,(\sin\gamma_j \quad \cos\gamma_j)\,\mathbf{F}_{\mathrm{fric}\ j} \tag{49}$$

$$0 = r_{\mathrm{r}j}\,(0 \quad 1)\,\mathbf{F}_{\mathrm{fric}\ j}, \tag{50}$$

with j from 1 to N_{c} (47), to N_{o} (48), to N (49) or to N_{s} (50). Note that (45) means that the resultant force produced by the frictional forces on the WMR is equal to the centripetal force necessary for the curvilinear motion; meanwhile (46) means that

there is equilibrium of moments on the WMR; and (50) means that the frictional force on the Swedish wheel j is zero in the roller longitudinal direction.

For a castor wheel j with no steering torque (free-steering) (47) results (51), with the meaning that its frictional force is zero in the direction perpendicular to the steering link:

$$\left| \begin{pmatrix} {}^{\mathrm{E}j}d_{\mathrm{S}jx} & {}^{\mathrm{E}j}d_{\mathrm{S}jy} & 0 \end{pmatrix}^{\mathrm{T}} \times \begin{pmatrix} \mathbf{F}^{\mathrm{T}}_{\mathrm{fric}\ j} & 0 \end{pmatrix}^{\mathrm{T}} \right| = 0. \tag{51}$$

In the same way, for a wheel j with no rotation torque (free-rotation) (49) results in (52), with the meaning that there is no frictional force in the direction defined by the wheel plane:

$$\begin{pmatrix} \sin\gamma_j & \cos\gamma_j \end{pmatrix} \mathbf{F}_{\mathrm{fric}\ j} = 0. \tag{52}$$

Note that a completely free castor/Swedish wheel (assuming that it is not singular, i.e. $\delta_i \neq 90°/\gamma_i \neq 0°$) has a null frictional force (i.e. no-slip) in the quasi-static motion model, due to equations (51)/(50) and (52).

3.5. Slip kinematic model

In the previous quasi-static motion model, the input variables $\mathbf{u}$ of (41) are the rotation torques $\tau_{\mathrm{ra}j}$ of all the non-free-rotation wheels and the steering torques $\tau_{\mathrm{csa}j}$ of all the non-free-steering castor wheels. Nevertheless, it is possible to directly consider the rotation and steering velocities $(\dot{\varphi}_{\mathrm{ra}j}, \dot{\beta}_{\mathrm{ca}j})$ of those non-free (i.e., assigned) wheels as the input variables $\mathbf{u}$ in (41), so that their associated equations (47) and (49), and torques could be obviated. Even, it is possible to consider WMR velocities as inputs (assigned) in the model. This leads to an inverse solution.

A generic 2-D frictional force is defined by:

$$\mathbf{F}_{\mathrm{fric}\ i} = -F_{\mathrm{N}i}\mathbf{f}_{\mathrm{fric}\ i}(\mathbf{v}_{\mathrm{slip}\ i}), \tag{53}$$

where $\mathbf{f}_{\mathrm{fric}\ i}$ is a generic 2-D function dependent on the vector sliding velocity.

This generic frictional force must be substituted in (45), (46), (50), (51) and (52). For example, it would produce in (50) null sliding velocity in the roller longitudinal direction. Therefore, afterwards this multiple substitution is carried out, the slip quasi-kinematic model is given by (45), (46), (50) (for all the Swedish wheels), (51) (for all the free-steering castor wheels) and (52) (for all the free-rotation wheels). Owing to the centripetal force on the left side of (45), this is a quasi-kinematic model with the assigned velocities as input variables. If the mentioned centripetal force is neglected, as is possible for smooth maneuvering (i.e., when ${}^{\bar{\mathrm{R}}}\mathbf{v}_{\mathrm{R}}$ and ${}^{\bar{\mathrm{R}}}\omega_{\mathrm{R}}$ do not have high values at the same time), it becomes a completely kinematic model— the slip kinematic model.

Note that when the centripetal force is neglected in the uniform curvilinear motion (quasi-static motion with respect to $\bar{\mathrm{R}}$) it is equivalent to the uniform rectilinear motion (quasi-static motion with respect to G). Therefore, for the slip kinematic model the normal reaction $F_{\mathrm{N}i}$ at the wheels remains constant and the origin of R

could be located arbitrarily (not necessary on the MC of the WMR*) since there is equilibrium of forces and moments.

3.6. Practical use of the slip kinematic model

There are three possible uses of the slip kinematic model depending on the assigned velocities:

- *Sensed wheel velocities are assigned.* The slip kinematic model is used as a forward solution to estimate the WMR movement with redundant sensor information.
- *Actuated wheel velocities are assigned.* The slip kinematic model is used as a forward solution to estimate the WMR movement with independently over-actuated wheel velocities. A simple example of this case is a 1-D WMR with two fixed wheels independently actuated.
- *WMR velocities are assigned.* The slip kinematic model is used as an inverse solution to compute the wheel velocities that produce a particular WMR movement. If the frictional force is well modeled this option increases the WMR mobility. For example, a tricycle WMR (two aligned fixed wheels and one orientable wheel) would have a full mobility through the rotation of the three wheels. Unlike the forward solution, for the inverse solution singularity may arise. In the example, a tricycle WMR with full mobility, singularity arises when the orientable wheel is parallel to the fixed wheels.

The second and third options are not very common in practice since it is not usual to assume slip as a working tool in order to increase the WMR mobility; meanwhile the first option is more usual, e.g., the slip kinematic equations could be used together with the EKF to estimate the WMR posture [7, 8].

3.7. Weighted LS solution of the kinematic model

The WMR no-slip kinematic constraints are given by (8). Applying a weighted matrix $\sqrt{\boldsymbol{\mu}}$ to (8):

$$\begin{pmatrix} \sqrt{\boldsymbol{\mu}_1} & \mathbf{0} & \cdots & \mathbf{0} \\ \mathbf{0} & \sqrt{\boldsymbol{\mu}_2} & \cdots & \vdots \\ \vdots & \vdots & \ddots & \mathbf{0} \\ \mathbf{0} & \cdots & \mathbf{0} & \sqrt{\boldsymbol{\mu}_{\mathrm{N}}} \end{pmatrix} \mathbf{A}\dot{\mathbf{q}} = \sqrt{\boldsymbol{\mu}}\mathbf{A}\dot{\mathbf{q}} = \mathbf{0}$$

$$\text{with } \sqrt{\boldsymbol{\mu}_i} = \begin{pmatrix} \sqrt{\mu_{xi}} & 0 \\ 0 & \sqrt{\mu_{yi}} \end{pmatrix}. \tag{54}$$

Separating the assigned velocities:

$$\sqrt{\boldsymbol{\mu}_{\mathrm{na}}}\mathbf{A}_{\mathrm{na}}\dot{\mathbf{q}}_{\mathrm{na}} = -\sqrt{\boldsymbol{\mu}_{\mathrm{a}}}\mathbf{A}_{\mathrm{a}}\dot{\mathbf{q}}_{\mathrm{a}}. \tag{55}$$

Computing the non-assigned velocities with the LS solution:

$$\dot{\mathbf{q}}_{\mathrm{na}} = -\left((\sqrt{\boldsymbol{\mu}_{\mathrm{na}}}\mathbf{A}_{\mathrm{na}})^{\mathrm{T}}\sqrt{\boldsymbol{\mu}_{\mathrm{na}}}\mathbf{A}_{\mathrm{na}}\right)^{-1}(\sqrt{\boldsymbol{\mu}_{\mathrm{na}}}\mathbf{A}_{\mathrm{na}})^{\mathrm{T}}\sqrt{\boldsymbol{\mu}_{\mathrm{a}}}\mathbf{A}_{\mathrm{a}}\dot{\mathbf{q}}_{\mathrm{a}}. \tag{56}$$

The singularity of the LS solution (56) is given by $\mathbf{A}_{\mathrm{na}}$ [13]. By definition, the LS algorithm minimizes the index J of (57), the sum of the quadratic error of the original equations, with respect to the non-assigned velocities:

$$J = (\sqrt{\boldsymbol{\mu}}\mathbf{A}\dot{\mathbf{q}})^{\mathrm{T}}(\sqrt{\boldsymbol{\mu}}\mathbf{A}\dot{\mathbf{q}}) = \dot{\mathbf{q}}^{\mathrm{T}}\mathbf{A}^{\mathrm{T}}\boldsymbol{\mu}\mathbf{A}\dot{\mathbf{q}} = \mathbf{v}_{\mathrm{slip}}^{\mathrm{T}}\boldsymbol{\mu}\mathbf{v}_{\mathrm{slip}}. \tag{57}$$

The minimizing (non-assigned) velocities could be the WMR linear velocity ${}^{\bar{\mathrm{R}}}\mathbf{v}_{\mathrm{R}}$, the WMR angular velocity ${}^{\bar{\mathrm{R}}}\omega_{\mathrm{R}}$, the steering velocity $\dot{\beta}_{\mathrm{c}j}$ of the castor wheel j the rotation velocity $\dot{\varphi}_j$ of the wheel j and the roller rotation velocity $\dot{\varphi}_{\mathrm{r}j}$ of the Swedish wheel j. The minimization of J with respect to those velocities, taking into account (1)–(3), (6) and (57), results:

$$\frac{\partial J}{\partial {}^{\bar{\mathrm{R}}}\mathbf{v}_{\mathrm{R}}} = \sum_{i=1}^{N}\mathbf{Rot}({}^{\mathrm{R}}\theta_{\mathrm{E}i})\boldsymbol{\mu}_i\mathbf{v}_{\mathrm{slip}\ i} = 0 \tag{58}$$

$$\frac{\partial J}{\partial {}^{\bar{\mathrm{R}}}\omega_{\mathrm{R}}} = \sum_{i=1}^{N}\left({}^{\mathrm{R}}\mathbf{d}_{\mathrm{E}i} \times \begin{pmatrix}\mathbf{Rot}({}^{\mathrm{R}}\theta_{\mathrm{E}i})\boldsymbol{\mu}_i\mathbf{v}_{\mathrm{slip}\ i}\\ 0\end{pmatrix}\right)\cdot\begin{pmatrix}0\\0\\1\end{pmatrix} = 0 \tag{59}$$

$$\frac{\partial J}{\partial \dot{\beta}_{\mathrm{c}j}} = -\left({}^{\mathrm{E}i}\mathbf{d}_{\mathrm{S}j} \times \begin{pmatrix}\boldsymbol{\mu}_j\mathbf{v}_{\mathrm{slip}\ j}\\ 0\end{pmatrix}\right)\cdot(0 \quad 0 \quad 1)^{\mathrm{T}} = 0 \tag{60}$$

$$\frac{\partial J}{\partial \dot{\varphi}_j} = r_j(\sin\gamma_j \quad \cos\gamma_j)\,\boldsymbol{\mu}_j\mathbf{v}_{\mathrm{slip}\ j} = 0 \tag{61}$$

$$\frac{\partial J}{\partial \dot{\varphi}_{\mathrm{r}j}} = r_{\mathrm{r}j}(0 \quad 1)\,\boldsymbol{\mu}_j\mathbf{v}_{\mathrm{slip}\ j} = 0. \tag{62}$$

For frictional forces (63) linearly dependent on the sliding velocities, there exist the following equivalences: (59)≡(46), (60)≡(51), (61)≡(52), (62)≡(50) and (58)≡(45) if the centripetal force on the left side of (45) is neglected:

$$\mathbf{F}_{\mathrm{fric}\ i} = -\begin{pmatrix}\mu_{xi} & 0\\ 0 & \mu_{yi}\end{pmatrix}\begin{pmatrix}v_{\mathrm{slip}\ xi}\\ v_{\mathrm{slip}\ xi}\end{pmatrix} = -\boldsymbol{\mu}_i\mathbf{v}_{\mathrm{slip}\ i}. \tag{63}$$

Note that the previous frictional force (63) neglects the coupling of the longitudinal and lateral coefficients. If they are considered coupled, using the anisotropy of the friction characteristics, it would produce a non-analytical solution for (56) or (58)–(62). For a proper physical sense of the weighted LS solution the WMR velocities must be considered non-assigned, so that the equilibrium of forces (58) and the equilibrium of moments (59) are always present. The wheel velocities may be assigned or non-assigned. Therefore, the weighted LS solution with the WMR velocities non-assigned is equivalent to the slip kinematic model with frictional forces linearly dependent on the sliding velocities.

4. APPLICATION OF KINEMATIC MODELING WITH SLIP

4.1. Tricycle WMR

In order to test the slip models of the previous section, we will consider the industrial forklift of Fig. 4. This vehicle represents a WMR close to real world. The slip models will be used as a forward solution to estimate the WMR movement, with the sensor information given by three encoders measuring the rotation of both fixed wheels (incremental encoders with 8290 pulses per revolution) and the orientation of the orientable wheel (absolute encoder with 1.41° resolution).

Figure 4 shows the tricycle equivalent representation with two fixed aligned wheels and other orientable wheel. Note that frame R has not been located on the MC of the WMR and ${}^{\mathrm{G}}\mathbf{v}_{\mathrm{MC}} \neq {}^{\mathrm{G}}\mathbf{v}_{\mathrm{R}}$, ${}^{\overline{\mathrm{MC}}}\omega_{\mathrm{MC}} = {}^{\bar{\mathrm{R}}}\omega_{\mathrm{R}}$, ${}^{\mathrm{G}}\theta_{\mathrm{MC}} = {}^{\mathrm{G}}\theta_{\mathrm{R}}$. From this graphical definition and using (2) 3 times, the slip kinematic equation (6) results:

$$\mathbf{v}_{\mathrm{slip}} = \begin{pmatrix} \mathbf{v}_{\mathrm{slip}\ 1} \\ \mathbf{v}_{\mathrm{slip}\ 2} \\ \mathbf{v}_{\mathrm{slip}\ 3} \end{pmatrix} = \left(\begin{array}{ccc|c} 1 & 0 & 0 & 0\ 0\ 0 \\ 0 & 1 & l_{12} & r\ 0\ 0 \\ \hline 1 & 0 & 0 & 0\ 0\ 0 \\ 0 & 1 & -l_{12} & 0\ r\ 0 \\ \hline \cos\beta_3 & \sin\beta_3 & l_3\cos\beta_3 & 0\ 0\ 0 \\ -\sin\beta_3 & \cos\beta_3 & -l_3\sin\beta_3 & 0\ 0\ r \end{array}\right) \begin{pmatrix} {}^{\bar{\mathrm{R}}}\dot{\mathbf{p}} \\ \dot{\varphi}_1 \\ \dot{\varphi}_2 \\ \dot{\varphi}_3 \end{pmatrix}. \tag{64}$$

The WMR dynamic equations, from (32)–(37), are:

$$\begin{aligned} & M_{\mathrm{T}}\,{}^{\mathrm{G}}\dot{\mathbf{v}}_{\mathrm{MC}} = \mathbf{Rot}({}^{\mathrm{G}}\theta_{\mathrm{R}})(\mathbf{F}_{\mathrm{fric}\ 1} + \mathbf{F}_{\mathrm{fric}\ 2} + \mathbf{Rot}(\beta_3)\mathbf{F}_{\mathrm{fric}\ 3}) \\ & I_{\mathrm{T}}\,{}^{\bar{\mathrm{R}}}\dot{\omega}_{\mathrm{R}} + I_{\mathrm{s}3}\ddot{\beta}_3 = (l_3 - l_{\mathrm{MC}})(F_{\mathrm{fric}\ x3}\cos\beta_3 - F_{\mathrm{fric}\ y3}\sin\beta_3) \\ & \qquad\qquad + l_{12}(F_{\mathrm{fric}\ y1} - F_{\mathrm{fric}\ y2}) - l_{\mathrm{MC}}(F_{\mathrm{fric}\ x1} + F_{\mathrm{fric}\ x2}) \\ & I_{\mathrm{r}1}\ddot{\varphi}_1 = \tau_{r1} + r\,(0 \quad 1)\,\mathbf{F}_{\mathrm{fric}\ 1}, \qquad I_{\mathrm{r}2}\ddot{\varphi}_2 = \tau_{r2} + r\,(0 \quad 1)\,\mathbf{F}_{\mathrm{fric}\ 2} \\ & I_{\mathrm{r}3}\ddot{\varphi}_3 = r\,(0 \quad 1)\,\mathbf{F}_{\mathrm{fric}\ 3}, \qquad I_{\mathrm{s}3}(\ddot{\beta}_3 + {}^{\bar{\mathrm{R}}}\dot{\omega}_{\mathrm{R}}) = \tau_{\mathrm{s}3}, \end{aligned} \tag{65}$$

where the orientable wheel is free in rotation. The quasi-static motion equations result in:

$$\begin{aligned} & M_{\mathrm{T}}\,{}^{\bar{\mathrm{R}}}\omega_{\mathrm{R}} \begin{pmatrix} 0 & -1 \\ 1 & 0 \end{pmatrix} {}^{\overline{\mathrm{MC}}}\mathbf{v}_{\mathrm{MC}} = (\mathbf{F}_{\mathrm{fric}\ 1} + \mathbf{F}_{\mathrm{fric}\ 2} + \mathbf{Rot}(\beta_3)\mathbf{F}_{\mathrm{fric}\ 3}) \\ & 0 = l_{12}(F_{\mathrm{fric}\ y1} - F_{\mathrm{fric}\ y2}) - l_{\mathrm{MC}}(F_{\mathrm{fric}\ x1} + F_{\mathrm{fric}\ x2}) \\ & \qquad + (l_3 - l_{\mathrm{MC}})(F_{\mathrm{fric}\ x3}\cos\beta_3 - F_{\mathrm{fric}\ y3}\sin\beta_3) \\ & 0 = \tau_{\mathrm{r}1} + r\,(0 \quad 1)\,\mathbf{F}_{\mathrm{fric}\ 1}, \qquad 0 = \tau_{\mathrm{r}2} + r\,(0 \quad 1)\,\mathbf{F}_{\mathrm{fric}\ 2} \\ & 0 = F_{\mathrm{fric}\ y3}, \qquad 0 = \tau_{\mathrm{s}3}. \end{aligned} \tag{66}$$

Therefore, the slip kinematic model is given by:

$$\begin{aligned} 0 &= F_{\mathrm{fric}\ x1} + F_{\mathrm{fric}\ x2} + F_{\mathrm{fric}\ x3}\cos\beta_3 \\ 0 &= F_{\mathrm{fric}\ y1} + F_{\mathrm{fric}\ y2} + F_{\mathrm{fric}\ x3}\sin\beta_3 \\ 0 &= l_{12}(F_{\mathrm{fric}\ y1} - F_{\mathrm{fric}\ y2}) + l_3 F_{\mathrm{fric}\ x3}\cos\beta_3. \end{aligned} \tag{67}$$

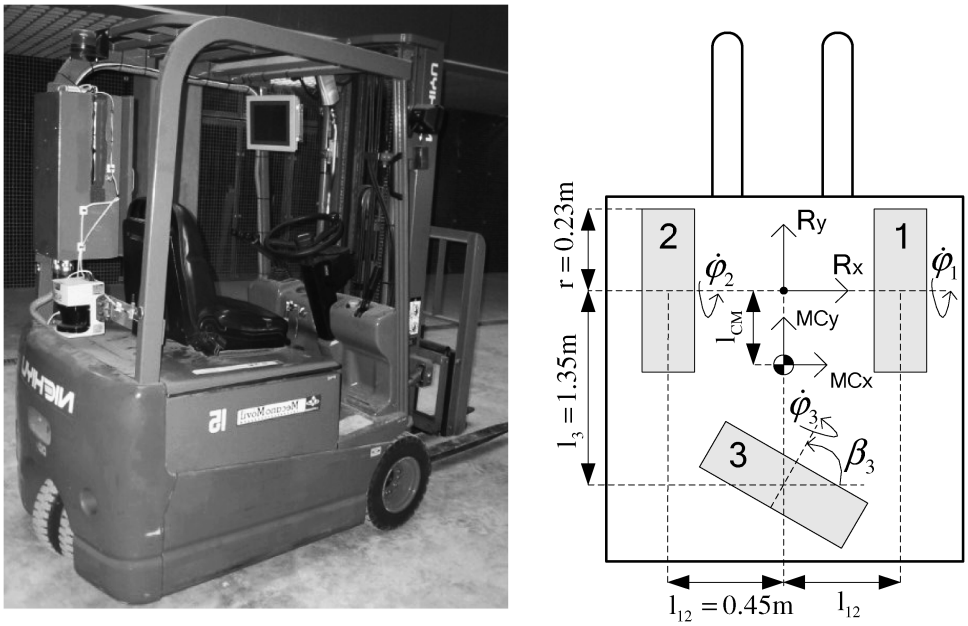

Figure 4. Industrial forklift Nichiyu FBT15 series 65 and top view with tricycle representation.

Moreover, for all the previous models ((65)–(67)) we have to include (53) 3 times, due to the frictional forces. The normal reactions on the wheels can be computed with:

$$\begin{aligned} &F_{\mathrm{N1}} + F_{\mathrm{N2}} + F_{\mathrm{N3}} = M_{\mathrm{T}} g \\ &l_{12}(F_{\mathrm{N1}} - F_{\mathrm{N2}}) + h_{\mathrm{MC}} M_{\mathrm{T}}{}^{\mathrm{MC,G}}\dot{v}_{\mathrm{MC}x} = 0 \\ &l_{\mathrm{MC}}(F_{\mathrm{N1}} + F_{\mathrm{N2}}) + h_{\mathrm{MC}} M_{\mathrm{T}}{}^{\mathrm{MC,G}}\dot{v}_{\mathrm{MC}y} = (l_3 - l_{\mathrm{MC}})F_{\mathrm{N3}} + \tau_{\mathrm{r1}} + \tau_{\mathrm{r2}}, \end{aligned} \tag{68}$$

where h_{MC} is the height of the MC with respect to the floor and ${}^{\mathrm{MC,G}}\dot{\mathbf{v}}_{\mathrm{MC}}$ is the acceleration (particularized for each model) of the MC with respect to frame G in coordinate frame MC.

On the other hand, (55) could be particularized to:

$$\begin{aligned} &\begin{pmatrix} \sqrt{2\mu_{x12}} & 0 & 0 \\ 0 & \sqrt{\mu_{y12}} & l_{12}\sqrt{\mu_{y12}} \\ 0 & \sqrt{\mu_{y12}} & -l_{12}\sqrt{\mu_{y12}} \\ \cos\beta_3\sqrt{\mu_{x3}} & \sin\beta_3\sqrt{\mu_{x3}} & l_3\cos\beta_3\sqrt{\mu_{x3}} \end{pmatrix} {}^{\bar{\mathrm{R}}}\dot{\mathbf{p}} \\ &= -\begin{pmatrix} 0 & 0 \\ r\sqrt{\mu_{y12}} & 0 \\ 0 & r\sqrt{\mu_{y12}} \\ 0 & 0 \end{pmatrix} \begin{pmatrix} \dot{\varphi}_1 \\ \dot{\varphi}_2 \end{pmatrix} \quad \longrightarrow \quad \mathbf{A}_{\boldsymbol{\mu}\mathrm{na}}\, {}^{\bar{\mathrm{R}}}\dot{\mathbf{p}} = -\mathbf{A}_{\boldsymbol{\mu}\mathrm{a}} \begin{pmatrix} \dot{\varphi}_1 \\ \dot{\varphi}_2 \end{pmatrix}, \end{aligned} \tag{69}$$

where (μ_{x12}, μ_{y12}) are the friction coefficients of the identical fixed wheels and μ_{x3} the friction coefficient of the orientable wheel in the L_{x3} direction. Note that (69)

considers together the first and third equation of (64), through a double value friction coefficient, and obviates the last equation, used only to compute $\dot{\varphi}_3$. Thus, the weighted LS solution is:

$$ {}^{\bar{\mathrm{R}}}\dot{\mathbf{p}} = -(\mathbf{A}_{\boldsymbol{\mu}\mathrm{na}}^{\mathrm{T}}\mathbf{A}_{\boldsymbol{\mu}\mathrm{na}})^{-1}\mathbf{A}_{\boldsymbol{\mu}\mathrm{na}}^{\mathrm{T}}\mathbf{A}_{\boldsymbol{\mu}\mathrm{a}}\begin{pmatrix}\dot{\varphi}_1\\ \dot{\varphi}_2\end{pmatrix}. \tag{70} $$

In order to compute this LS solution we have to know the three friction coefficients, or simply two relationships between them through the constants k_{11} and k_{12}:

$$ \begin{aligned} \mu_{y12} &= k_{11}\mu_{x12}\\ \mu_{x3} &= k_{12}\mu_{x12}. \end{aligned} \tag{71} $$

4.2. Estimation of the WMR velocity vector with the KF

The discrete state and output equations are:

$$ {}^{\bar{\mathrm{R}}}\dot{\mathbf{p}}_{k+1} = {}^{\bar{\mathrm{R}}}\dot{\mathbf{p}}_k + T\,{}^{\bar{\mathrm{R}}}\ddot{\mathbf{p}}_k \tag{72} $$

$$ \begin{pmatrix}\dot{\varphi}_1 r\\ \dot{\varphi}_2 r\\ 0\end{pmatrix}_k = \begin{pmatrix}0 & -1 & -l_{12}\\ 0 & -1 & l_{12}\\ \cos\beta_3 & \sin\beta_3 & l_3\cos\beta_3\end{pmatrix}_k {}^{\bar{\mathrm{R}}}\dot{\mathbf{p}}_k \rightarrow \mathbf{y}_{1k} = \mathbf{C}_{1k}\,{}^{\bar{\mathrm{R}}}\dot{\mathbf{p}}_k, \tag{73} $$

where k is the time step considered and T the sample time. The output equation (73) has three elements, one for each sensor, obtained from the no-slip kinematics of (64). Note that β_3 in the third scalar equation of (73) has not been made explicit since it would force us to work with the extended KF that uses a first-order approximation. That approximation is not required with the approach of (73). Nevertheless (73), although it has one scalar equation for each sensor (as usual), does not include all the kinematic of (69), since it lacks the first element. In order to avoid this, an alternative approach for the output equation is:

$$ \begin{pmatrix}0\\ \dot{\varphi}_1 r\\ \dot{\varphi}_2 r\\ 0\end{pmatrix}_k = \begin{pmatrix}1 & 0 & 0\\ 0 & -1 & -l_{12}\\ 0 & -1 & l_{12}\\ \cos\beta_3 & \sin\beta_3 & l_3\cos\beta_3\end{pmatrix}_k {}^{\bar{\mathrm{R}}}\dot{\mathbf{p}}_k \rightarrow \mathbf{y}_{2k} = \mathbf{C}_{2k}\,{}^{\bar{\mathrm{R}}}\dot{\mathbf{p}}_k. \tag{74} $$

The KF that uses (73) will be denoted as KF1 and the KF that uses (74) as KF2. The second-order time derivative term of (72) will be considered as the process noise in the state equation, where the state matrix is the identity matrix. Thus, the recursively equations of the KF result in:

$$ {}^{\bar{\mathrm{R}}}\hat{\dot{\mathbf{p}}}_{k+1/k} = {}^{\bar{\mathrm{R}}}\hat{\dot{\mathbf{p}}}_{k/k} \tag{75} $$

$$ \mathbf{P}_{k+1/k} = \mathbf{P}_{k/k} + \mathbf{Q}_k \tag{76} $$

$$ \mathbf{K}_{k+1} = \mathbf{P}_{k+1/k}\mathbf{C}_{k+1}^{\mathrm{T}}(\mathbf{C}_{k+1}\mathbf{P}_{k+1/k}\mathbf{C}_{k+1}^{\mathrm{T}} + \mathbf{R}_{k+1})^{-1} \tag{77} $$

$$ {}^{\bar{\mathrm{R}}}\hat{\dot{\mathbf{p}}}_{k+1/k+1} = {}^{\bar{\mathrm{R}}}\hat{\dot{\mathbf{p}}}_{k+1/k} + \mathbf{K}_{k+1}(\mathbf{y}_{k+1} - \mathbf{C}_{k+1}\,{}^{\bar{\mathrm{R}}}\hat{\dot{\mathbf{p}}}_{k+1/k}) \tag{78} $$

$$ \mathbf{P}_{k+1/k+1} = (\mathbf{I} - \mathbf{K}_{k+1}\mathbf{C}_{k+1})\mathbf{P}_{k+1/k}, \tag{79} $$

where $\mathbf{C}_k = \mathbf{C}_{1k}$ or $\mathbf{C}_{2k}$, $\mathbf{y}_k = \mathbf{y}_{1k}$ or $\mathbf{y}_{2k}$, k is the time step, $\mathbf{Q}_k$ is the process noise covariance matrix, $\mathbf{R}_k$ is the measurement noise covariance matrix, $\mathbf{K}_k$ is the gain matrix and $\mathbf{P}_k$ is the error covariance matrix. The noise covariance matrices will be assumed constant. Note that the proposed KF is very simple since the state equation (75) predicts the previous state value, which is corrected with the measurements in (78). In general, it will be considered the covariance matrices:

$$\begin{aligned} &\mathbf{Q} = k_{13}^2\mathbf{I}, \qquad \mathbf{R} = \mathbf{R}_1 \text{ or } \mathbf{R}_2 \\ &\mathbf{R}_1 = \begin{pmatrix} k_{14}^2 & 0 & 0 \\ 0 & k_{14}^2 & 0 \\ 0 & 0 & k_{15}^2 \end{pmatrix} \\ &\mathbf{R}_2 = \begin{pmatrix} k_{16}^2 & 0 & 0 & 0 \\ 0 & k_{17}^2 & 0 & 0 \\ 0 & 0 & k_{17}^2 & 0 \\ 0 & 0 & 0 & k_{18}^2 \end{pmatrix}, \end{aligned} \tag{80}$$

where both encoders of the fixed wheels and the scalar state equations have been supposed equally confidence through the standard deviations k_{14}/k_{17} and k_{13}, and the errors of the variables have been assumed uncorrelated. In order to apply the KF two/three parameters of (80) have to be established, e.g., $\{k_{14}, k_{15}\}/\{k_{16}, k_{17}, k_{18}\}$, if the other one is fixed, e.g., $k_{13} = 1$, without loss of generality. Note that it is not possible to use a stationary solution of the KF, which would be given by the stationary correction matrix $\mathbf{K}_\infty$ and equation (78), since the output matrix $\mathbf{C}_k$ is variable.

4.3. Experimental results

For this paper it has been considered worthy to focus on experimental results rather than on simulation. Nevertheless, it would be possible to compare through simulation the dynamic model (65) with the three slip models [(66), (67) and (70)] once the model parameters have been established (estimated, identified, conjectured, etc.). Naturally, the simulation results would show that (67) is more accurate than (70) and less than (66). Here we will consider the third approximation level of the dynamic model (weighted LS) since this can be computed analytically. This slip model will be compared with the KF1 and KF2, and with the classical odometric model of the differential drive WMR (DM):

$${}^{\bar{\mathrm{R}}}\dot{\mathbf{p}}_k = \begin{pmatrix} 0 & 0 \\ -r/2 & -r/2 \\ -r/(2l_{12}) & r/(2l_{12}) \end{pmatrix} \begin{pmatrix} \dot{\varphi}_{1k} \\ \dot{\varphi}_{2k} \end{pmatrix}. \tag{81}$$

This comparison will be done on the basis of the paths obtained with each model, through the numerical integration of ${}^{\bar{\mathrm{R}}}\dot{\mathbf{p}}$, for several experiments. These experiments will be carried out in such a way that the real final WMR posture $\mathbf{p}(\infty)$ exactly fits the initial WMR posture $\mathbf{p}(0)$. In order to establish the values of the slip

model parameters $\{k_{11}, k_{12}\}$, the KF1 parameters $\{k_{14}, k_{15}\}$ and the KF2 parameters $\{k_{16}, k_{17}, k_{18}\}$, the following error index J will be minimized:

$$J = \frac{1}{2N_e} \sum_{i=1}^{N_e} \left(\frac{\sqrt{(x_\infty - x_0)^2 + (y_\infty - y_0)^2}}{\text{distance traveled}} + \frac{|\theta_\infty - \theta_0|}{\text{angle traveled}} \right), \tag{82}$$

where N_e is the number of experiments considered.

For the optimization of the slip/KF1/KF2 model parameters we have considered 15 experiments, realized in parking at medium velocity of around 2 m/s. In particular, we have used (82) together with the Matlab® function lsqnonlin specifying a maximum number of iterations, a minimum tolerance, the range of the parameter values and the initialization of the search.

For the slip model, after the optimization process, we obtain $k_{11} = 3.2 \times 10^{-3}$, $k_{12} = 19.2$ and $J_{\min} = 2.02\%$. The parameter values obtained show that the fixed wheels have less confidence in the longitudinal direction, i.e., their associated equations are less accurate. This is logical since the fixed wheels are the traction wheels and the traction is mainly produced, except for non-smooth maneuvering, in the longitudinal direction. For small slip the longitudinal slip increases with the traction force, see Fig. 3. Obviously the traction forces on the fixed wheels are coordinated by the control target of the forklift with the orientation of the orientable wheel. Figure 5 shows the path obtained with the slip model when tracking approximately a rectangle, while Fig. 6 shows the values measured by the sensors for this experiment.

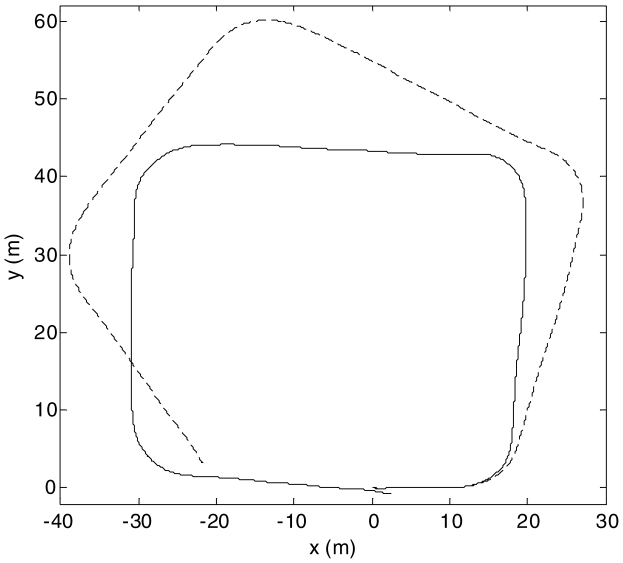

Figure 5. Path obtained with the optimized (—-) and non-optimized (- -) ($k_{11} = 0.32$, $k_{12} = 2$, $J = 11.55\%$) slip model when tracking a rectangle.

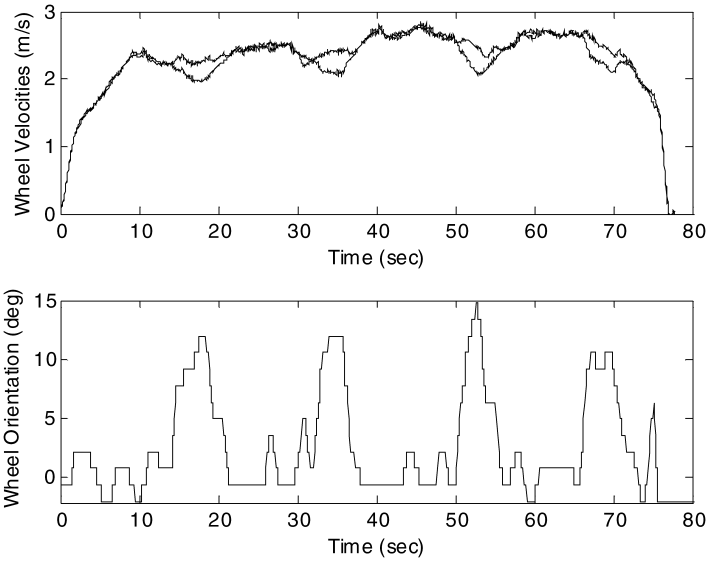

Figure 6. Measured velocities of the fixed wheels ($-r\dot{\varphi}_1$, $-r\dot{\varphi}_2$) and measured orientation β_3 of the orientable wheel for the rectangle experiment.

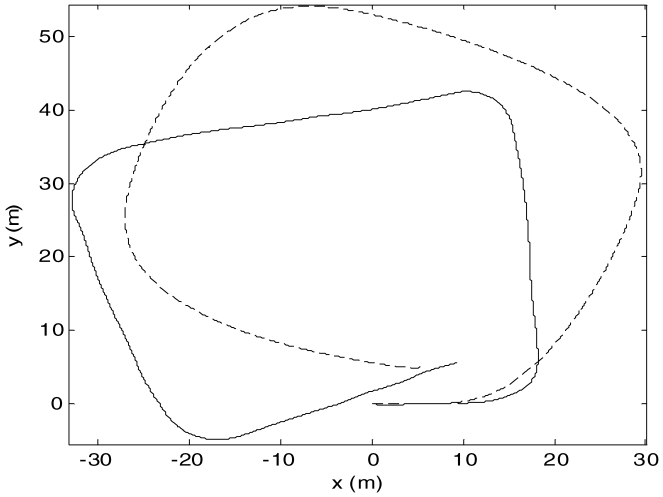

Figure 7. Path obtained with the optimized (—-) and non-optimized (- -) ($k_{14} = k_{15} = 200$, $J = 12.16\%$) KF1 when tracking a rectangle.

For the KF1, after the optimization process, it is obtained $k_{14} = 0.31$, $k_{15} = 1.09$ and $J_{\min} = 7.11\%$. These parameter values imply that the rotation of the fixed wheels is filtered a little and that the orientation β_3 is quite filtered. Figure 7 shows the path obtained with the KF1 for the rectangle experiment. For the KF2, after the optimization process, we obtain $k_{16} = 0.28$, $k_{17} = 3.57$, $k_{18} = 0.28$ and $J_{\min} = 2.1\%$. These parameter values imply that the rotation of both fixed wheels

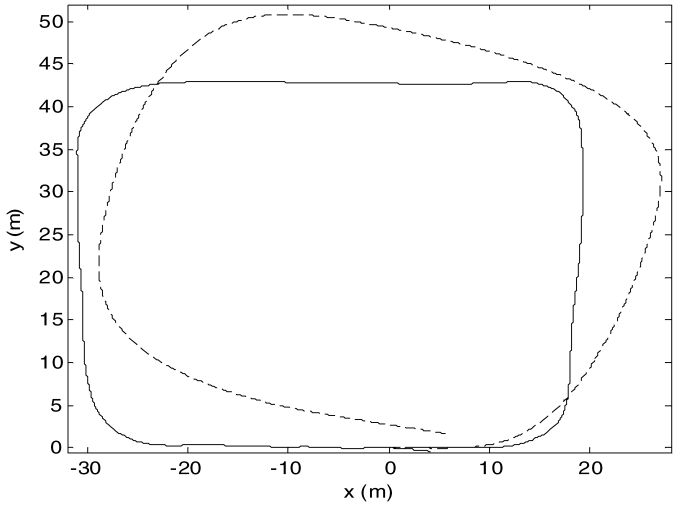

Figure 8. Path obtained with the optimized (——) and non-optimized (- -) ($k_{16} = k_{17} = k_{18} = 200$, $J = 6.85\%$) KF2 when tracking a rectangle.

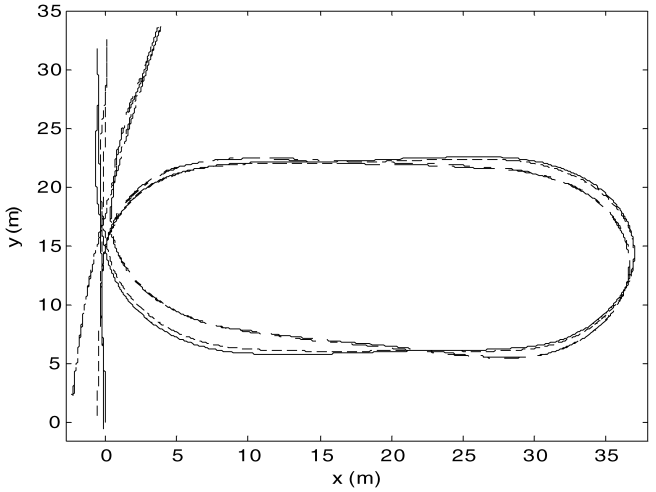

Figure 9. Second tracking path: slip model (——), KF1 (– –), KF2 (- -) and DM (– · –).

are much filtered, and that the orientation β_3 and the equation ${}^{\bar{\mathrm{R}}}v_{\mathrm{R}x} = 0$ are filtered just a little. This qualitatively agrees with the values of the WLS. Figure 8 shows the path obtained with the KF2 for the rectangle experiment.

Figures 9–12 show the paths obtained with the slip model (——), the KF1 (– –), the KF2 (- -) and the DM (– · –) for other experiments. In particular, the fifth tracking path (Fig. 12) is the most critical since the angle traveled (accumulated rotation motion) is $3 \times 360°$. In fact, the KF1 and the DM clearly fail in the path estimation while the slip model and the KF2 keep a pretty good estimation. For all the experiments the slip model and the KF2 give better results than the KF1 and the DM

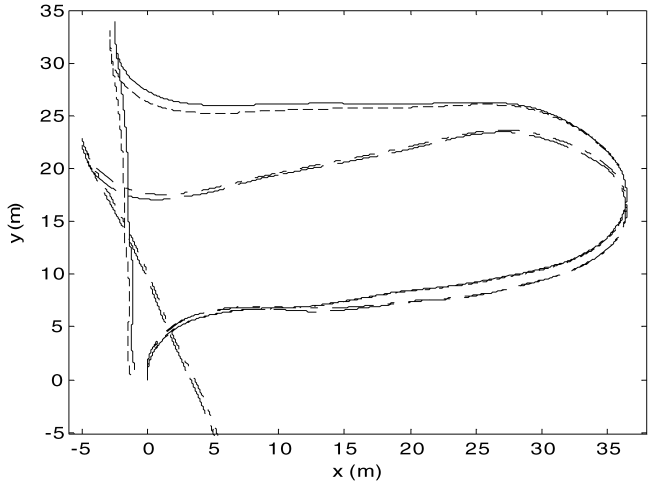

Figure 10. Third tracking path: slip model (—-), KF1 (– –), KF2 (- -) and DM (– · –).

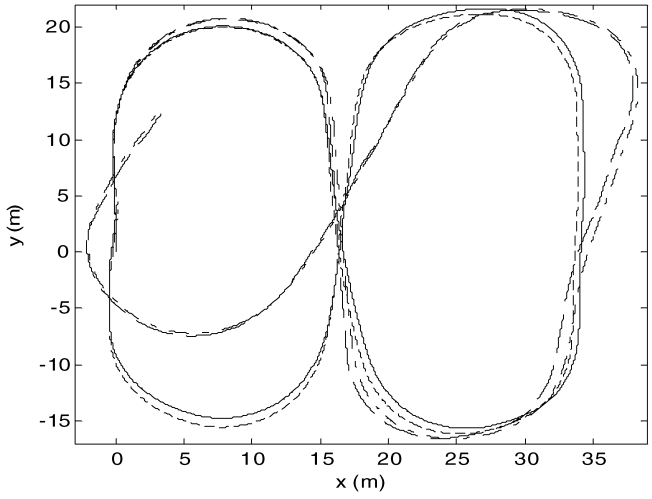

Figure 11. Fourth tracking path: slip model (—-), KF1 (– –), KF2 (- -) and DM (– · –).

($J = 7.14\%$). In general, the KF2/KF1 results are similar to the slip model/DM. Nevertheless, the slip model/DM takes 16.5%/98.5% less computational time than the KF2/KF1 (see Table 4).

Figure 13 shows the interface developed (path obtained with the slip model, indicators, buttons, etc.) with LabVIEW software for the touch panel incorporated to the industrial forklift.

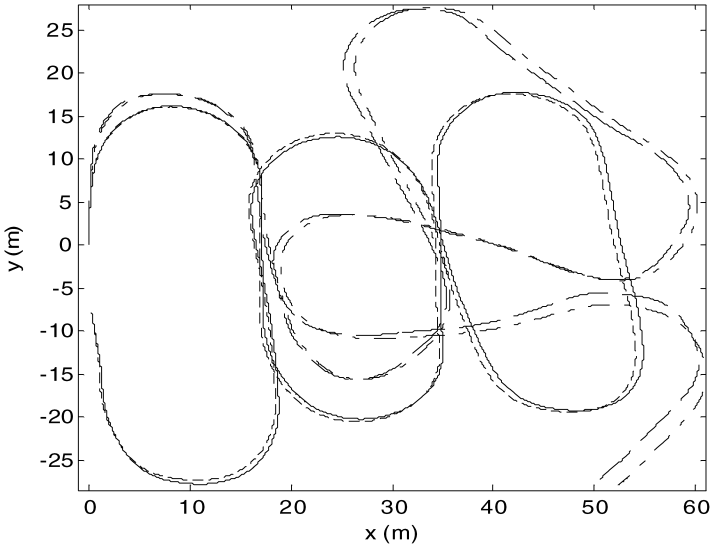

Figure 12. Fifth tracking path: slip model (—-), KF1 (– –), KF2 (- -) and DM (– · –).

Table 4.
Computational cost of the models

Parameter	Slip model	KF2	DM	KF1
Additions	30	131	3	102
Products	102	255	6	180
Inverse matrices	1 of 3×3	1 of 4×4	0	1 of 3×3
Time[a] (ns)	46	55	0.8	51

[a] Obtained with Matlab on Pentium M (1.6 GHz).

5. CONCLUSION AND FURTHER WORK

The main contribution of this research is the three kinematic models with slip presented in Section 3. Unlike others [4–7] (Section 3.1), these models have been obtained from physical principles, i.e., from successive approximations of the WMR dynamics.

The first approximation level of the dynamic approach consists of considering a WMR quasi-static motion with respect to the body coincident frame, which is equivalent to a WMR uniform curvilinear motion with a constant angular velocity, as well as neglecting the mass of the castor wheels.

Furthermore, the second approximation level neglects the centripetal force required for the WMR curvilinear motion, which is possible for smooth maneuvering. The model obtained is completely kinematic: the slip kinematic model.

Moreover, the third approximation level considers frictional forces linearly dependent on the sliding velocities. The resultant slip model is equivalent to the weighted LS solution of the WMR no-slip kinematics, where the WMR velocities must be

Figure 13. Interface of the touch panel incorporated to the industrial forklift.

considered non-assigned. The advantage of the third approximation level is that the model is computed analytically, although it is less accurate due to the three approximations. However, any of the three slip models could be used through numerical computation.

An industrial forklift, equivalent to a tricycle WMR, has been used in a real situation to validate the slip model of the third approximation level. In particular, it has been shown that the experimental results for this slip model greatly improve the ones obtained with the first proposed Kalman filter and the differential-drive model. This slip model results similar to the second proposed Kalman filter, but it takes approximately 16% less computational time.

It is conclude that the proposed WMR slip modeling is straightforwardly applicable for both simulation and real situations. For that purpose, first we must obtain the kinematic and dynamic model of the WMR and, second, the friction functions and/or parameters must be determined, based on theoretical principles or on experimental data, e.g., with the simple optimization method used in Section 4.3.

It is suggested as further work to integrate the developed kinematic models with slip within kinematic and dynamic control schemes.

Acknowledgments

This work was supported in part by the Spanish Government: research projects DPI2000-0362-P4-05, DPI2004-07417-C04-01 and BIA2005-09377-C03-02.

REFERENCES

1. R. M. Murray and S. S. Sastry, Nonholonomic motion planning: steering using sinusoids, *IEEE Trans. Automatic Control* **38**, 700–716 (1993).
2. C. Canudas de Wit and O. J. Sordalen, Exponential stabilization of mobile robots with nonholonomic constraints, in: *Proc. IEEE Conf. on Decision and Control*, Brighton, pp. 692–697 (1991).
3. E. Badreddin and M. Mansour, Fuzzy-tuned state-feedback control of a nonholonomic mobile robot, in: *Proc. 12th World Congr. of the IFAC*, Sidney, vol. 6, pp. 577–580 (1993).
4. P. F. Muir and C. P. Neuman, Kinematic modeling of wheeled mobile robots, *J. Robotic Syst.* **4** 281–329 (1987).
5. J. C. Alexander and J. H. Maddocks, On the kinematics of wheeled mobile robots, *Int. J. Robotics Res.* **8**, 15–27 (1989).
6. W. Kim, B.-J. Yi and D. J. Lim, Kinematic modeling of mobile robots by transfer method of augmented generalized coordinates, *J. Robotic Syst.* **21**, 301–322 (2004).
7. Y. K. Tham, H. Wang and E. K. Teoh, Adapttive state estimation for 4-wheel steerable industrial vehicles, in: *Proc. 37th IEEE Conf. on Decision and Control*, Tampa, FL, pp. 4509–4514 (1998).
8. S. Scheding, G. Dissanayake, E. M. Nebot and H. Durrant-Whyte, An experiment in autonomous navigation of an underground mining vehicle, *IEEE Trans. Robotics Automat.* **15** 85–95 (1999).
9. G. Campion, G. Bastin and B. D'Andrea-Novel, Structural properties and classification of kinematic and dynamic models of wheeled mobile robots, *IEEE Trans. Robotics Automat.* **12**, 47–61 (1996).
10. R. Rajagopalan, A generic kinematic formulation for wheeled mobile robots, *J. Robotic Syst.* **14**, 77–91 (1997).
11. K. H. Low and Y. P. Leow, Kinematic modeling, mobility analysis and design of wheeled mobile robots, *Adv. Robotics* **19**, 73–99 (2005).
12. B.-J. Yi and W. K. Kim, The kinematics for redundantly actuated omnidirectional mobile robots, *J. Robotic Syst.* **19**, 255–267 (2002).
13. L. Gracia and J. Tornero, Kinematic modeling and singularity of wheeled mobile robots, *Adv. Robotics* **21**, 793–816 (2007).
14. E. Routh, *Dynamics of a System of Rigid Bodies*, *Part 1*, 7th edn. Macmillan, New-York (1905).
15. H. Dugoff, P. S. Fancher ans L. Segel, An analysis of tire traction properties and their influence on vehicle dynamic performance, SAE Paper 7000377 (1970).
16. M. G. Bekker, *Off-The-Road Locomotion*. University of Michigan Press, Ann Arbor, MI (1960).
17. J. Okello, M. J. Dwyer and F. B. Cottrell, The tractive performance of rubber tracks and a tractor driving wheel tyre as influenced by design parameters, *J. Agric. Eng. Res.* **59**, 33–43 (1994).
18. H. B. Pacejka and E. Bakker, The 'magic formula' tyre model, *Vehicle Syst. Dyn.* **21**, 1–18 (1993).
19. H. B. Pacejka and I. J. M. Besselink, Magic formula tyre model with transient properties, *Vehicle Syst. Dyn. Suppl.* **27**, 234–249 (1997).
20. N. Matsumoto and M. Tomizuka, Vehicle lateral velocity and yaw rate control with two independent control inputs, *ASME J. Dyn. Syst. Meas. Control* **114**, 606–613 (1992).
21. H. S. Tan and Y.-K. Chin, Vehicle traction control: variable structure control approach, *ASME J. Dyn. Syst. Meas. Control* **113**, 223–230 (1991).

22. R. Stribeck, Die wesentlichen Eigenschaften der Gleit- und Rollenlager [The key qualities of sliding and roller bearings], *Z. Vereines Seutscher Ing.* **46** (38, 39), 1342–1348 and 1432–1437 (1902).
23. P. Dahl, A solid friction model, *Technical Report TOR-0158H3107–18I-1*, Aerospace Corporation, El Segundo, CA (1968).
24. P.-A. Bliman and M. Sorine, Friction modelling by hysteresis operators: application to Dahl, sticktion and Stribeck effects, in: *Proc. Conf. on Models of Hysteresis*, Trento, pp. 10–19 (1991).
25. C. Canudas de Wit, H. Olsson, K. J. Åström and P. Lischinsky, A new model for control of systems with friction, *IEEE Trans. Automatic Control* **40**, 419–425 (1995).
26. D. Karnopp, Computer simulation of slip-stick friction in mechanical dynamic systems, *AMSE J. Dyn. Syst. Meas. Control* **107**, 100–103 (1985).
27. E. Velenis, P. Tsiotras, C. Canudas-de-Wit and M. Sorine, Dynamic tyre friction models for combined longitudinal and lateral vehicle motion, *Vehicle Syst. Dyn.* **43**, 3–29 (2005).
28. H. B. Pacejka, *Tyre and Vehicle Dynamics*. Butterworth-Heinemann, Oxford (2002).

ABOUT THE AUTHORS

Luis Gracia received the BS degree in Electronic Engineering, the MS degree in Control Systems Engineering, and the PhD in Automation and Industrial Computer Science from the Technical University of Valencia (UPV), Spain, in 1998, 2000 and 2006, respectively. He held a PhD Fellowship for 1 year at the Department of Systems Engineering and Control of the UPV, where he has been employed as an Assistant Professor since 2002. He was awarded both the BS and MS degrees with the First Spanish National Prize.

Josep Tornero received the MS degree in Systems and Control from the University of Manchester, Institute of Science and Technology in 1982, and the PhD in Electrical Engineering at the UPV, Spain, in 1985. He is currently Professor at the Department of Systems Engineering and Control at the UPV. He has been Visiting Professor at the CIRSSE (NASA Center for Intelligent Robotics Systems for Space Exploration), the Rensselaer Polytechnic Institute at Troy (New York) and at the Department of Mechanical Engineering at the University of California (Berkeley). He is presently responsible for the 'Automation in Manufacture and Mobile Robotics' Group and the 'Design Institute for the manufacture and automated production', both at the UPV. He is particularly interested in modeling, control and simulation of auto-guided-vehicles and robot arms; modeling, analysis and control of multirate sampled data systems; and collision detection/avoidance and automatic trajectory generation. He has participated in many European research projects such as ESPRIT, BRITE, EUREKA and STRIDE, and in educational projects such as ERAMUS, INTERCAMPUS, ALPHAS and TEMPUS.